Proceedings of the Combustion Institute 41 (2025) 105839

Contents lists available at ScienceDirect

Proceedings of the Combustion Institute

journal homepage: www.elsevier.com/locate/proci

Techno-economic analysis of deep peaking for hydrogen co-firing in a 300 MWe subcritical power plant with hydrogen production from valley electricity

Tiantian Wang [a], Jinwei Sun [a], Fuqi Yuan [a], Mingye Yang [a], Yang Zhang [b,*], Fuyuan Yang [a,*], Minggao Ouyang [a]

[a] School of Vehicle and Mobility, Tsinghua University, Beijing 100084, China
[b] Key Laboratory for Thermal Science and Power Engineering of Ministry of Education, Department of Energy and Power Engineering, Tsinghua University, Beijing 100084, China

ARTICLE INFO

Keywords:
Coal-fired power plant
Deep peaking
Hydrogen production
Valley electricity
Hydrogen co-firing

ABSTRACT

As the proportion of renewable power generation increases annually, thermal power plants are supposed to operate in deep peaking with high flexibility to balance power supply and power demand as well as ensure grid security. Hydrogen co-firing in thermal power plants is one of the promising approaches to maintaining stable combustion during deep peaking periods, improving peak capacity, and reducing carbon emissions. This paper numerically investigated the thermodynamic performance of deep peaking at 30 % and 20 % heating loads for hydrogen co-firing in a 300 MWe subcritical power plant using the Aspen Plus model and conducted an economic analysis of four scenarios of boiler deep peaking and hydrogen production from valley electricity. The results show that as the hydrogen blending heat ratio increases from 0 % to 15 % with the constant total excess air ratio of 1.15 at 30 % heating load, the boiler thermal efficiency increases from 91.13 % to 92.05 %, the standard coal consumption decreases from 395 g/kWh to 331 g/kWh, and the CO_2 emission per unit of fuel heat input also drops from 132.52 g/MJ to 112.55 g/MJ. If the boiler heating load is further adjusted to 20 %, hydrogen blending and oxygen enrichment can also improve the theoretical combustion temperature and boiler efficiency, as well as save coal and reduce carbon emissions. Regarding the economic analysis, the prices of standard coal and electrolyzers are two key factors affecting the payback time. As the capacity of electrolyzers decreases from 60 MW in Scenario 2 to 20 MW in Scenario 4, the payback time drops from 10.45 years to 3.63 years. In the meantime, the hydrogen blending heat ratio also decreases from 15 % to 5 % at 20 % heating load. There exists a tradeoff between a high hydrogen blending ratio (which means more stable combustion at low heating loads) and a short payback time.

1. Introduction

According to the Global Energy Review 2025, the share of coal-fired power generation is almost 60 % in China in 2024, which makes the power industry one of the major contributors to carbon emissions [1]. To realize the carbon neutrality goal, the proportion of renewable energy, such as wind and solar energy, in power generation is increasing annually [2]. However, due to the fluctuation, intermittency, and randomness of power generation from renewable energy [3], this requires coal-fired power plants to operate in deep peaking with a high degree of flexibility to balance power supply and power demand as well as ensure grid security. Under this circumstance, steady combustion of coal-fired power plants at low heating loads is a key issue. The blending of gas fuels such as hydrogen, ammonia, and methane is one of the approaches to solve the above problem [4–6].

Hydrogen co-firing in thermal power plants not only helps to maintain stable combustion at low heating loads due to its high reactivity but also favors carbon reduction [7], which has gradually become a research hotspot in recent years. Some researchers have investigated the effect of hydrogen addition on gas-fired boilers, focusing on combustion stability [8], thermodynamic performance [9–10], pollutant emissions [11–12], etc. In the meantime, several studies of hydrogen co-firing in coal-fired

* Corresponding authors.
E-mail addresses: yang-zhang@tsinghua.edu.cn (Y. Zhang), fyyang@mail.tsinghua.edu.cn (F. Yang).

https://doi.org/10.1016/j.proci.2025.105839
Received 20 June 2025; Accepted 4 September 2025
Available online 20 September 2025

boilers have also been carried out. Ueki et al. [13] experimentally investigated the effect of hydrogen gas addition on the combustibility of pulverized coal using a drop tube furnace. It was found that the combustibility of coal was enhanced with an optimum hydrogen gas flow. Yao et al. [14] analyzed the effects of coupling hydrogen-derived fuels with coal on the thermodynamic parameters of a 300 MW tangentially fired boiler through thermal calculations, it was found that boiler thermodynamic parameters depended on the properties of hydrogen-derived fuels and coupling mass percentage, the coal consumption rate dropped after the large proportion of cofiring, thus the CO_2 emission reduced. Wei et al. [15] numerically studied hydrogen co-firing in a 660 MW power plant concerning combustion stability, heat transfer, and NOx formation through computational fluid dynamics (CFD). If hydrogen is injected into the boiler from two layers of secondary air nozzles with a hydrogen mixing ratio of 40 %, the boiler heat flow is 1.04 times higher, and the NOx mass slightly increases at the furnace exit, about 1.13 times.

Moreover, some researchers focused on strategies for reducing cycling costs and improving the peak capacity of coal-fired power plants through power to gas. Romeo et al. [16] proposed an integration system of a Power to Gas (PtG) module (50 MWe) with fossil fuel thermal power plants (500 MWe) to reduce the minimum complaint load and avoid shutdowns. The utilization of PtG diminished the specific cost of producing electricity between 20 % and 50 %. Arslan et al. [17] designed a multi-generation system including power generation, domestic hot water, and hydrogen production for the waste heat recovery of a 150 MW coal-fired power plant. The results showed that an increase of 15.78–16.53 % in energy efficiency was achieved. Fu et al. [18] proposed a novel oxy-fuel power plant coupled with both liquid O_2 storage and cold energy recovery systems to adapt to the peak-shaving requirements.

According to the aforementioned literature, hydrogen co-firing in thermal power plants is a promising approach to improving peak capacity and reducing carbon emissions. However, the effects of hydrogen addition on the thermodynamic parameters of coal-fired boilers at low heating loads are rarely studied. This work aims to numerically investigate the thermodynamic performance of deep peaking for a 300 MWe subcritical coal-fired power plant with hydrogen blending combustion through Aspen Plus software [19–20], which is commonly used for thermodynamic process simulation in thermal power plants. Additionally, an economic analysis is conducted to discuss the costs of hydrogen production from valley electricity and the benefits of coal saving and carbon reduction from hydrogen blending combustion. This paper can provide a reference for the deep peaking operation of thermal power plants.

2. Methods

2.1. 300 MWe boiler setup

Fig. 1 is the simplified diagram of a 300 MWe subcritical coal-fired boiler. It mainly includes two loops, which are the fuel-air-flue gas loop and the water-steam loop. In the fuel-air-flue gas loop, coal is crushed into powder in coal mills, dried, and fed into the furnace for combustion with the preheated air. After combustion, the ash from the combustion products is gathered and discharged from the furnace via the dry bottom hopper. The high-temperature flue gas flows through the furnace and subsequent heat transfer surfaces and finally exits the boiler. It is worth mentioning that the flue gas desulphurization, denitrification, and dedusting processes are not considered in the study.

In the water-steam loop, the pumped water flows through the economizer, boiler drum, water wall, low-temperature superheater, platen superheater and wing wall, and high-temperature superheater, and finally becomes the superheated steam flowing into the high-pressure turbine to generate electricity. After working in the high-pressure turbine, both the temperature and pressure of the steam

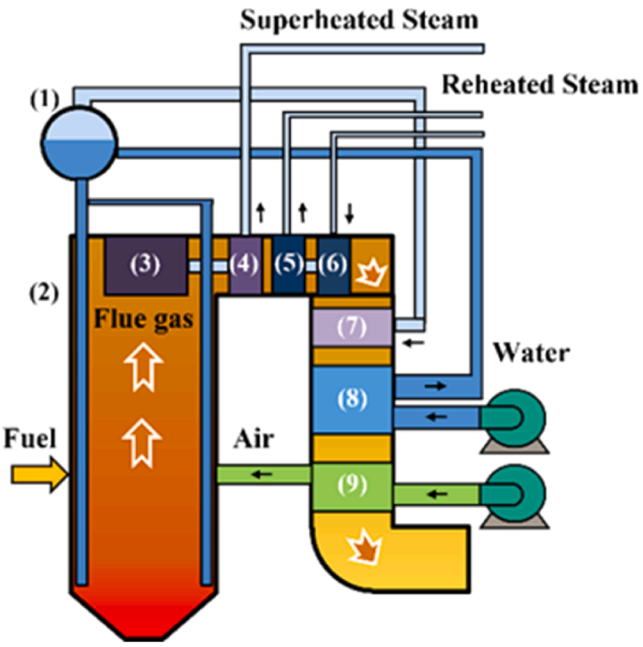

Fig. 1. Simplified diagram of a 300 MWe coal-fired boiler.
(1) boiler drum; (2) water wall; (3) platen superheater and wing wall; (4) high-temperature superheater; (5) high-temperature reheater; (6) low-temperature reheater; (7) low-temperature superheater; (8) economizer; (9) air preheater.

drop, and then it is sent back to the boiler, heated by the flue gas in the low-temperature reheater and high-temperature reheater, and finally becomes the reheated steam flowing into the intermediate-pressure and low-pressure turbines to generate electricity. After working in those components, the steam is condensed and pumped to the economizer to start a new cycle.

The coal type in this study is lignite, the detailed ultimate and proximate analyses are shown in Table 1.

The designed parameters for the 300 MWe subcritical coal-fired boiler (HG-1035/17.5-HM35) in China from the 30 % boiler maximum continuous rating (BMCR) case to the 100 % BMCR case are listed in Table 2. According to the boiler design manual, the boiler can be adjusted from 30 % to 100 % of the heating load. Additionally, the ultimate and proximate analyses of the lignite in Table 1 are the design fuel parameters for this boiler.

2.2. Aspen Plus model of the 300 MWe power plant

The established Aspen Plus model of the 300 MWe thermal power plant is illustrated in Fig. 2. The simulation of coal combustion is divided into four processes, including coal drying (Rstoic & Flash module), pyrolysis (RYield module), combustion (RGibbs module), and flue gas and ash separation (Cyclone module). Coal is defined as a non-conventional

Table 1
Detailed ultimate and proximate analyses of the lignite in this study.

Parameters (units)		Value
Ultimate analysis	Carbon (wt. %)	62.15
	Hydrogen (wt. %)	5.06
	Oxygen (wt. %)	15.04
	Nitrogen (wt. %)	1.10
	Sulphur (wt. %)	0.66
Proximate analysis	Ash (wt. %)	15.99
	Moisture (wt. %)	29.60
	Volatile (wt. %)	26.10
	Fixed carbon (wt. %)	28.31
Lower heat value (MJ/kg)		14.51

Table 2
Designed thermodynamic parameters for the 300 MWe subcritical coal-fired boiler.

Parameters (units)	100 % BMCR case	75 % BMCR case	50 % BMCR case	30 % BMCR case
The mass flow rate of superheated steam (t/h)	1035	776.25	517.50	310.50
Superheated steam pressure at the boiler exit (MPa(g))	17.5	17.09	12.86	7.23
Superheated steam temperature at the boiler exit (°C)	540	540	536	523
Feed water pressure (MPa (g))	19.39	18.30	13.90	8.23
Feed water temperature (°C)	282.8	264.7	241.6	217.6
The mass flow rate of reheated steam (t/h)	846.8	646.9	441.6	263.9
Reheated steam pressure at the boiler exit (MPa(g))	3.816	2.902	1.936	1.125
Reheated steam temperature at the boiler exit (°C)	540	540	523	506
Reheated steam pressure at the boiler inlet (MPa(g))	3.996	3.039	2.030	1.201
Reheated steam temperature at the boiler inlet (°C)	333.5	306.5	297.9	293.9

component in the simulation process, the enthalpy and density of coal are calculated by the HCOALGEN model and the DCOALIGT model. The products of coal pyrolysis are C, H_2, O_2, N_2, S, and ash. The yield of each product is dynamically linked to the input coal ultimate analysis and proximate analysis using the Fortran language. After the Cyclone model, the heat exchanges between the flue gas and working fluid are calculated according to the HeatX module, which includes thermodynamic and heat transfer calculations, and the heat exchanges between the flue gas and air are calculated according to the MheatX module, which can complete multi-stream thermodynamic equilibrium calculations.

The thermal efficiency of the coal-fired boiler can be obtained according to Eq. (1).

$$\eta_{th} = Q_s / Q_f \quad (1)$$

where Q_s indicates the absorbed heat of superheated steam and reheated steam, and Q_f indicates the supplied heat of fuel entering the boiler.

The generating efficiency of the entire thermal power plant can be assessed according to Eq. (2).

$$\eta_e = Q_e / Q_f \quad (2)$$

where Q_e indicates the generated electricity of the superheated and reheated steam.

The thermodynamic parameter comparison between the simulated values and the designed values in the 100 % BMCR case is shown in Table 3 to demonstrate the reliability of the Aspen Plus model.

The errors of these parameters are within ±1 % except for electricity generation, which is −3.96 %. It should be noted that the values of the isentropic efficiency of three turbines and the neglect of pipeline pressure drop and heat loss may be the reasons for the error in electricity generation of the power plant [21].

2.3. Aspen Plus model of the 20 MW electrolyzer

Subsequently, the electrolyzer module is introduced to simulate the 20 MW alkaline electrolyzer, as shown in Fig. 3. It is adapted to the valley electricity input from the power plant, and is more cost-effective than proton exchange membrane (PEM) electrolyzer and solid oxide water electrolysis (SOEC).

The alkaline electrolyzer parameters are listed in Table 4. The previous study [22] investigated the Aspen Plus model of an alkaline electrolysis system for hydrogen production, which provides references for this study. For example, the recommended range for alkaline electrolyzer efficiency is generally from 56 % to 70 % [23–24], thus, the electrolyzer efficiency is set at 65 % with 100 % load. The calculated specific energy consumption is 51.3 kWh/kg H_2.

3. Results and discussion

3.1. Thermodynamic performance of the 300 MWe power plant under different heating loads

Fig. 4 demonstrates that as the boiler heating load reduces from 100 % to 30 % with the constant excess air ratio of 1.15, the combustion temperature in the furnace drops, thus the flue gas temperature at the furnace outlet decreases, and the exhaust gas temperature also slightly reduces. Under such circumstances, the boiler thermal efficiency drops

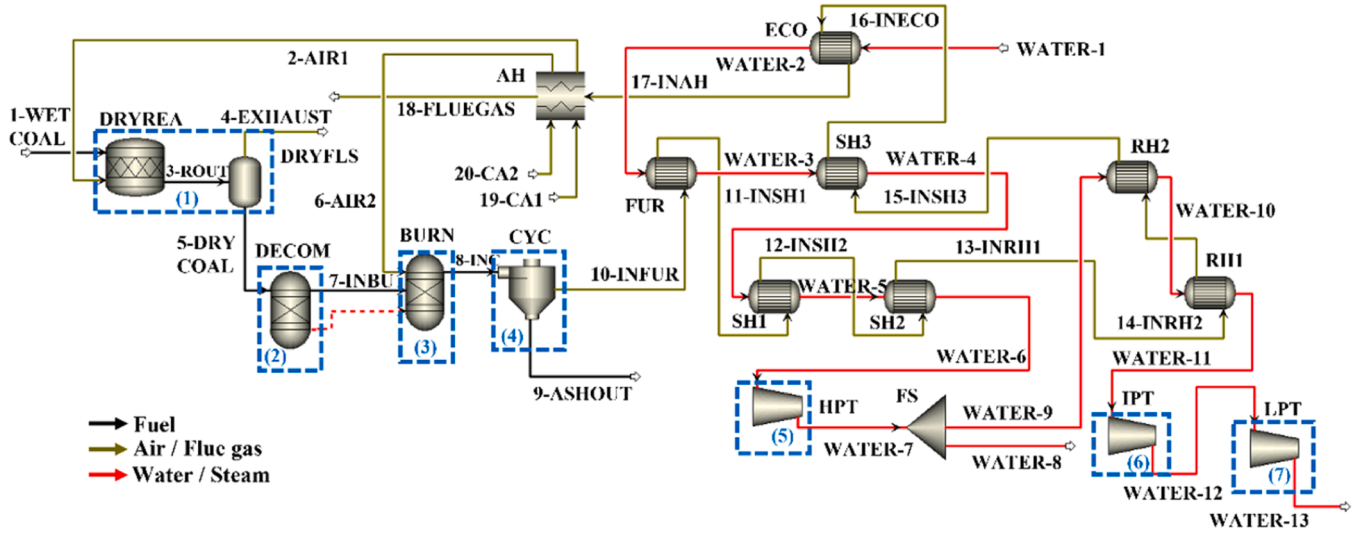

Fig. 2. Aspen Plus model of a 300 MWe thermal power plant.
(1) coal drying; (2) coal pyrolysis; (3) coal combustion; (4) flue gas and ash separation; (5) high-pressure turbine (HPT); (6) intermediate-pressure turbine (IPT); (7) low-pressure turbine (LPT).

Table 3
Thermodynamic parameter comparison between simulated values and designed values in the 100 % BMCR case.

Parameters (units)	Designed value	Simulated value	Errors
The mass flow rate of superheated steam (t/h)	1035	1035	–
Superheated steam pressure at the boiler exit (MPa(g))	17.5	17.5	–
Superheated steam temperature at the boiler exit (°C)	540	541.1	0.20 %
The mass flow rate of reheated steam (t/h)	846.8	846.8	–
Reheated steam pressure at the boiler exit (MPa(g))	3.816	3.816	–
Reheated steam temperature at the boiler exit (°C)	540	537.2	−0.52 %
Reheated steam pressure at the boiler inlet (MPa(g))	3.996	3.996	–
Reheated steam temperature at the boiler inlet (°C)	333.5	337.0	0.75 %
Exhaust gas temperature (°C)	144.4	144.1	−0.21 %
Thermal efficiency of the boiler (%)	92.41	92.49	0.09 %
Electricity energy generation (MW)	335.343	322.048	−3.96 %

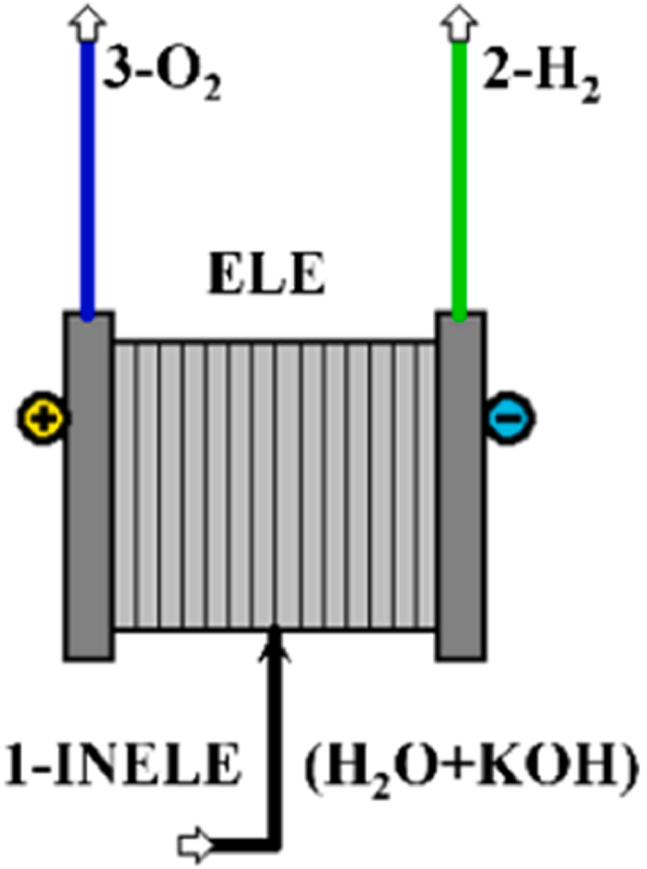

Fig. 3. Aspen Plus model of a 20 MW alkaline electrolyzer.

from 92.49 % to 91.13 %, and the overall generating efficiency of the thermal power plant decreases from 40.80 % to 31.11 %.

Fig. 5 shows that as the boiler heating load decreases from 100 % to 30 %, the CO_2 emission per unit of fuel heat input rises from 129.83 g/MJ to 132.52 g/MJ and the standard coal consumption increases from 301 g/kWh to 395 g/kWh due to the decrease in the thermal efficiency of the boiler and the generating efficiency of the thermal power plant.

Table 4
Parameters of the alkaline electrolyzer.

Parameters (units)	Value
Operating temperature (°C)	75.75
Operating pressure (bar)	7
Electrolyte concentration (wt. % KOH)	35
Input power (MW)	20
Energy efficiency (LHV) (%)	65 [22–23]
Voltage (V)	1.93
Hydrogen yield (kg/h)	390.1
Oxygen yield (kg/h)	3096.4
Energy consumption (kWh/kg H_2)	51.3

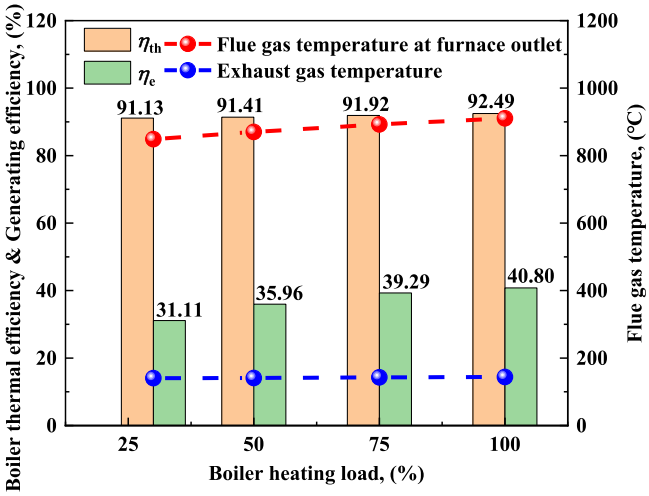

Fig. 4. Key boiler parameters under different heating loads.

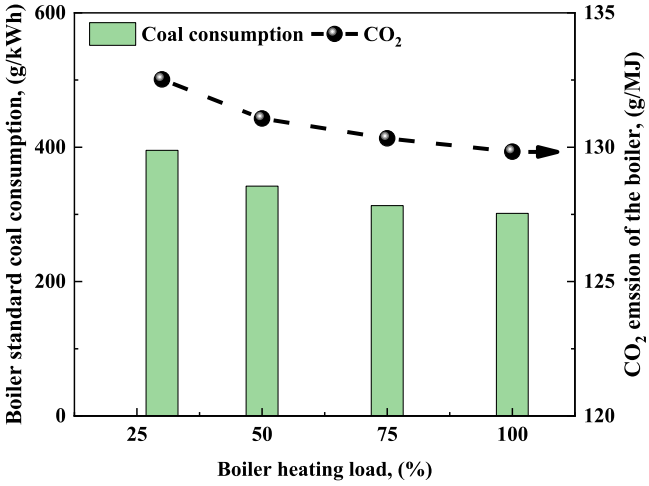

Fig. 5. Coal consumption and CO_2 emissions of the boiler under different heating loads.

Additionally, the variation of gas components in the boiler exhaust gas is further discussed in **the S1 section of *Supplemental Material***. In this study, the NOx concentration (6 % O_2) is 284 mg/Nm^3 in the 30 % BMCR case according to the zero-dimensional model in Aspen Plus. The pollutant order of magnitude is basically consistent with published studies [7,15].

3.2. Thermodynamic performance of the 300 MWe power plant with hydrogen co-firing

Based on the online data from the Shandong Power Trading Centre in China, the renewable energy output and real-time electricity price of the Shandong power grid in two typical days are shown in Fig. 6. In this study, 9:00 to 15:00 (6 h) is considered on average as the high incidence of renewable energy power (green line in Fig. 6) in a day. Meanwhile, the real-time electricity price (black line in Fig. 6) decreases to below 200 CNY/MWh, or even a negative price. It is worth mentioning that the average valley electricity window (6 h/d) may apply to the North China and East China regions, which are geographically close to Shandong Province. While it may vary in other Chinese regions due to the different wind and solar resource endowments.

If it is considered to adjust the boiler to 30 % heating load during low electricity price hours, at the same time, hydrogen is produced from valley electricity, and then it is used for co-firing at 30 % low heating load of the 300 MWe boiler, which has the combined benefits of saving coal and reducing carbon emissions. The detailed strategy is to carry out boiler deep peaking for 6 h a day, the boiler heating load decreases to 30 %, and this part of the generated valley electricity is used for hydrogen production by water electrolysis, which requires four 20 MW alkaline electrolyzers. Subsequently, the produced hydrogen is sent to the boiler for co-firing at 30 % heating load, and the highest hydrogen blending heat ratio can be up to 15 %. In the meantime, if the oxygen produced by water electrolysis is also used for oxy-fuel combustion, the air supply based on the 15 % hydrogen blending condition decreases to maintain the same excess air ratio. The oxygen content in the air sent to the furnace can increase from 21 % to 22.4 %.

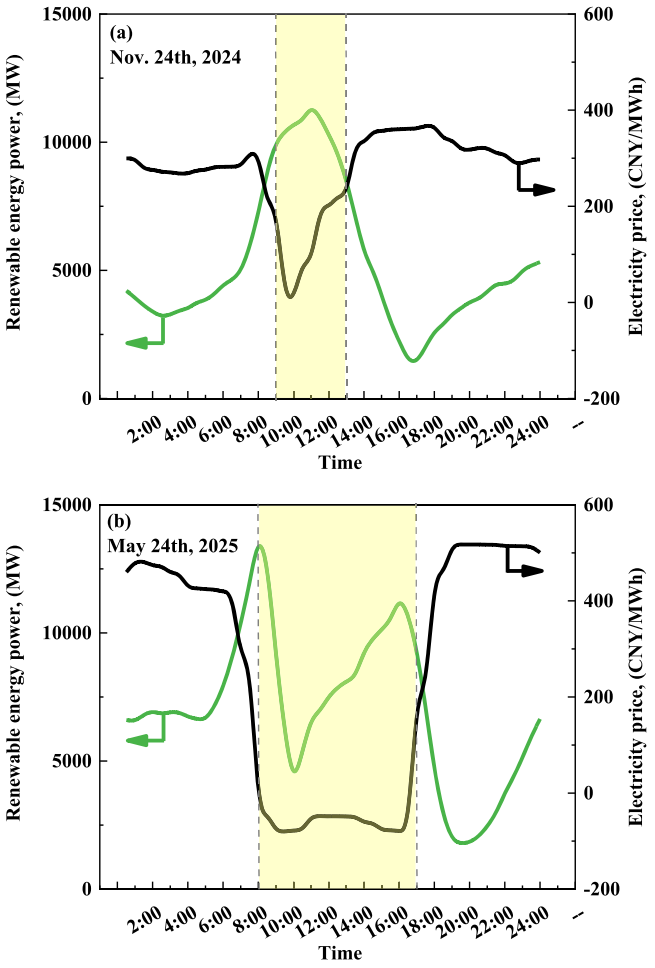

Fig. 6. Renewable energy output and real-time electricity price of the Shandong power grid.

Fig. 7 shows that as the hydrogen blending ratio increases from 0 % to 15 % with the constant total excess air ratio of 1.15, the theoretical combustion temperature in the furnace rises from 1514 °C to 1578 °C, while the flue gas temperature at the furnace outlet decreases. Under such circumstances, the boiler thermal efficiency increases from 91.13 % to 92.05 %, and the overall generating efficiency of the thermal power plant rises from 31.11 % to 31.63 %. As for oxy-fuel combustion alongside hydrogen blending, the theoretical combustion temperature rises from 1578 °C to 1634 °C. Generally speaking, oxy-fuel combustion increases the reaction rate and combustion temperature and shortens the ignition delay time, which benefits the combustion stability [25]. However, the increase in combustion temperature caused by oxygen enrichment may result in the risk of wall temperature exceedance or corrosion inside the boiler [26].

Considering hydrogen injection and oxygen enrichment, the hydrogen and oxygen supply system and leakage detection devices are necessary in practice. The burners should be added or modified for hydrogen diffusion combustion in the furnace. It is required to evaluate whether the furnace, heat transfer surface, and flue gas treatment system need to be modified based on the hydrogen blending ratio or oxygen concentration to ensure the safe and efficient operation of the boiler.

Fig. 8 indicates that as the hydrogen blending heat ratio increases from 0 % to 15 %, the standard coal consumption decreases from 395 g/kWh to 331 g/kWh and the CO_2 emission per unit of fuel heat input also drops from 132.52 g/MJ to 112.55 g/MJ due to the combined effects of coal saving and energy efficiency improvement.

Additionally, the NOx concentration (6 % O_2) generally increases from 284 mg/Nm^3 to 409 mg/Nm^3 as the hydrogen blending ratio rises from 0 % to 15 %. This trend is consistent with published studies [7,15]. Considering the increase in NOx emissions after hydrogen blending, it is recommended to optimize the combustion organization of hydrogen and coal in the furnace, adjust the air staged combustion strategy, and add flue gas recirculation in order to eliminate high-temperature zones and control NOx generation from the source [27]. Meanwhile, NOx emissions can also be controlled through optimizing flue gas post-treatment (*e.g.*, denitrification) while ensuring stable combustion at low loads [28]. Further discussion can be found in **the S2 section of *Supplemental Material***.

Since hydrogen blending and oxygen enrichment benefit stable combustion at low heating loads, which can increase the combustion temperature and boiler efficiency, it is further considered that the boiler heating load is adjusted from 30 % to 20 % during the deep peaking

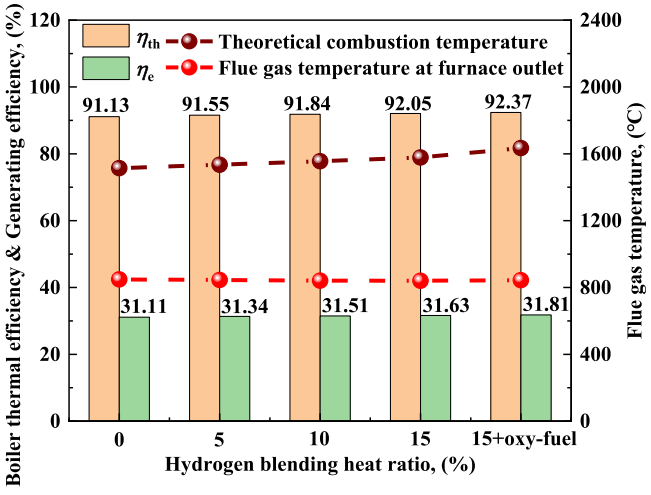

Fig. 7. Key boiler parameters under different hydrogen blending heat ratios at 30 % boiler heating load.

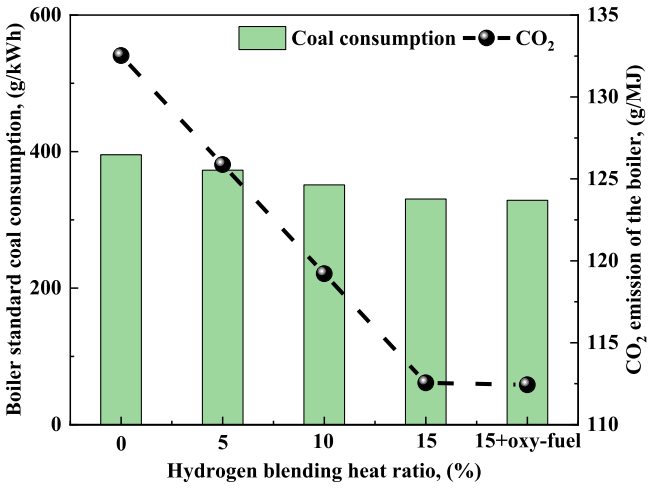

Fig. 8. Coal consumption and CO_2 emissions of the boiler under different heating loads at 30 % boiler heating load.

period [29], which is currently the advanced level of deep peaking technology on the boiler side of thermal power plants.

If the boiler heating load decreases to 20 %, the valley electricity is used for hydrogen production by water electrolysis, which requires three 20 MW alkaline electrolyzers. The produced hydrogen and oxygen are sent to the boiler for combustion at a 20 % heating load case. Similarly, the highest hydrogen blending heat ratio can be up to 15 %, and the oxygen content in the air can increase to 22.4 %.

Fig. 9 illustrates the thermodynamic parameter changes under different cases at 20 % boiler heating load. The results show that hydrogen blending and oxygen enrichment can improve the theoretical combustion temperature and boiler efficiency, as well as save coal and reduce carbon emissions.

3.3. Economic analysis of the 300 MWe power plant with hydrogen co-firing

Based on the thermodynamic calculation, four scenarios of 300-day deep peaking of the boiler per year and hydrogen production from valley electricity are discussed in this chapter, these are 1) 6-hour deep peaking to 30 % heating load per day, with all valley electricity used for hydrogen production; 2) 6-hour deep peaking to 20 % heating load per day, with all valley electricity used for hydrogen production; 3) 6-hour deep peaking to 20 % heating load per day, with two-thirds of valley electricity used for hydrogen production; 4) 6-hour deep peaking to 20 % heating load per day, with one-third of valley electricity used for hydrogen production.

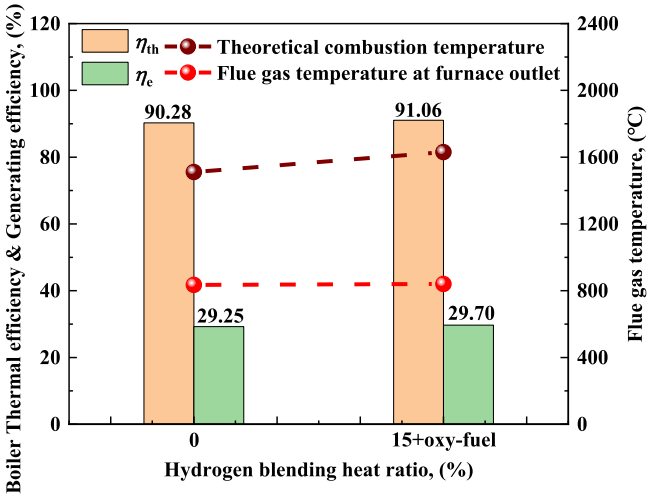

Fig. 9. Key boiler parameters under different hydrogen blending heat ratios at 20 % boiler heating load.

The cost and benefit comparisons of these four scenarios are listed in Table 5. The costs mainly include capital expenditures (CapEx), annual operating expenditures (OpEx), annual electricity costs for hydrogen production, and annual water consumption costs. The benefits mainly include annual coal savings and carbon reduction. As for Scenario 1, the capital expenditures are expensive, meanwhile, annual coal saving and carbon reduction benefits are insufficient to cover annual operating expenditures, electricity costs, and consumed water costs, which is not acceptable. Regarding Scenarios 2–4, as the capacity of electrolyzers decreases from 60 MW to 20 MW, the final payback time drops from 10.45 years to 3.63 years. Additionally, it is noteworthy that the hydrogen blending heat ratio also decreases from 15 % to 5 % as the capacity of electrolyzers decreases from 60 MW in Scenario 2 to 20 MW in Scenario 4.

The potential targets for cost reduction and benefit improvement are further discussed in **the S3 section of *Supplemental Material***, which indicates that the prices of standard coal and electrolyzers are two vital parameters affecting the payback time.

4. Conclusion

In this study, the steady-state thermodynamic performance of deep peaking at 30 % and 20 % heating loads for hydrogen co-firing in a 300 MWe subcritical power plant was numerically investigated using the Aspen Plus model, and the economic analysis of four scenarios of boiler deep peaking and hydrogen production from valley electricity was conducted. The main conclusions are as follows:

(1) The coal-fired boiler itself can achieve 30 % to 100 % heating load regulation. As the boiler heating load reduces from 100 % to 30 % with the constant total excess air ratio of 1.15, the boiler thermal efficiency and the overall generating efficiency both decrease while the standard coal consumption and the CO_2 emission slightly increase.

(2) Considering the boiler heating load adjusts to 30 % with hydrogen blending and oxygen enrichment combustion, as the hydrogen blending heat ratio increases from 0 % to 15 % with the constant total excess air ratio of 1.15, the boiler thermal efficiency increases from 91.13 % to 92.05 %, the standard coal consumption decreases from 395 g/kWh to 331 g/kWh, and the CO_2 emission also drops from 132.52 g/MJ to 112.55 g/MJ. If the boiler heating load is further adjusted to 20 %, hydrogen blending and oxygen enrichment can also improve the boiler efficiency, as well as save coal and reduce carbon emissions.

(3) As for the economic analysis, the prices of standard coal and electrolyzers are two vital parameters affecting the payback time. As the capacity of electrolyzers decreases from 60 MW to 20 MW, the final payback time drops from 10.45 years to 3.63 years. Meanwhile, the hydrogen blending heat ratio also decreases from 15 % to 5 % at 20 % heating load. The tradeoff exists between a high hydrogen blending ratio (which means more stable combustion at low heating loads) and a short payback time.

Finally, it is worth mentioning that the dynamic performance in terms of load-following behavior and combustion characteristics is essential in real-world applications, which will be further investigated in future work.

Novelty and significance statement

The novelty of this research is the comprehensive thermodynamic and economic analysis of deep peaking for hydrogen co-firing in a 300

Table 5
Economic comparison of four scenarios of boiler deep peaking and hydrogen production from valley electricity.

Parameters (units)		Scenario 1	Scenario 2	Scenario 3	Scenario 4
CapEx (CNY)	Electrolyzer	160,000,000	120,000,000	80,000,000	40,000,000
	(2000 CNY/kW [30,31])	(80 MW)	(60 MW)	(40 MW)	(20 MW)
	Hydrogen storage tank	12,800,000	9600,000	6400,000	3200,000
	(320 CNY/m^3 [32])	(20,000 m^3 × 2)	(15,000 m^3 × 2)	(10,000 m^3 × 2)	(5000 m^3 × 2)
	Burners and pipes	25,000,000	25,000,000	25,000,000	25,000,000
	Total	197,800,000	154,600,000	111,400,000	68,200,000
OpEx (CNY, 2 % of CapEx [33])		3956,000	3092,000	2228,000	1364,000
Hydrogen production electricity costs (CNY, the valley electricity price is 100 CNY/MWh)		14,400,000	10,800,000	7200,000	3600,000
Consumed water costs (CNY, water consumption is 0.204 ton/MWh [30], industrial tap water price is 5 CNY/ton [30])		146,880	110,160	73,440	36,720
Standard coal savings (tons per year)		10,474	29,994	27,376	24,757
Coal saving benefits (CNY, standard coal price is 700 CNY/ton)		7332,000	20,996,000	19,163,000	17,330,000
CO_2 emission reduction (tons per year, 2.6 tons of CO_2 from 1 ton of standard coal)		27,232	77,985	71,177	64,369
Carbon reduction benefits (CNY, carbon tax is 100 CNY/ton)		2723,200	7798,500	7117,700	6436,900
Payback time (year)		None	10.45	6.64	3.63

MWe subcritical coal-fired power plant with hydrogen production from valley electricity. The route proposed in this study has proved to be technically and economically feasible. It is significant because this research discusses a potential environment-friendly and cost-efficient decarbonization approach in the thermal power industry, which contributes to the achievement of the dual-carbon goal in China.

CRediT authorship contribution statement

Tiantian Wang: Writing – original draft, Software, Methodology, Investigation. **Jinwei Sun:** Software, Methodology. **Fuqi Yuan:** Software, Methodology. **Mingye Yang:** Software, Investigation. **Yang Zhang:** Writing – review & editing, Supervision. **Fuyuan Yang:** Supervision, Funding acquisition. **Minggao Ouyang:** Supervision, Conceptualization.

Declaration of competing interest

The authors declare that they have no known competing financial interests or personal relationships that could have appeared to influence the work reported in this paper.

Acknowledgements

This work was jointly supported by the National Key R&D Program of China (2023YFB4005501), the Huaneng Group Science and Technology Research Project (HNKJ24-HF05), and Ordos National Sustainable Development Agenda Innovation Demonstration Zone Construction Science and Technology Support Project (KCX2024009).

Supplementary materials

Supplementary material associated with this article can be found, in the online version, at doi:10.1016/j.proci.2025.105839.

References

[1] J. Xie, Z. Liang, X.B. Zhang, L. Zhu, J. Clean. Prod. 222 (2019) 573–583.
[2] M.K.G. Deshmukh, M. Sameeroddin, D. Abdul, M. Abdul Sattar, Mater. Today: Proc 80 (2023) 1756–1759.
[3] M. Mahdavi, F. Jurado, K. Schmitt, M. Chamana, IEEE T. Ind. Appl. 60 (2024) 3543–3553.
[4] D. Hong, Y. Guo, C. Wang, T. Xu, S. Ma, P. Combust. Inst. 40 (2024) 105678.
[5] H. Khalid, I. Ryo, H. Genya, X. Yu, H. Nozomu, F. Osamu, P. Combust. Inst. 38 (2021) 4131–4139.
[6] M. Xia, D. Zabrodiec, P. Scouflaire, B. Fiorina, N. Darabiha, P. Combust. Inst. 36 (2017) 2123–2130.
[7] D. Wei, Z. Zhang, Y. Wang, Z. Zhu, L. Wu, T. Wang, Energy 305 (2024) 132336.
[8] X. Yang, T. Wang, Y. Zhang, H. Zhang, Y. Wu, J. Zhang, Energy 239 (2022) 122248.
[9] T. Wang, X. Liu, Y. Zhang, H. Zhang, Appl. Energ. 358 (2024) 122614.
[10] T. Wang, H. Zhang, Y. Zhang, H. Wang, J. Lyu, G. Yue, Int. J. Hydrogen Energ. 47 (2022) 28188–28203.
[11] M.K. Büyükakin, S. Öztuna, Int. J. Hydrogen Energ. 45 (2020) 35246–35256.
[12] S. Öztuna, M.K. Büyükakin, Int. J. Hydrogen Energ. 45 (2020) 5971–5986.
[13] Y. Ueki, R. Yoshiie, I. Naruse, S. Matsuzaki, Fuel Process. Technol. 161 (2017) 289–294.
[14] Q. Yao, R. Li, Y. Wang, Y. Li, L. Zhang, L. Deng, D. Che, Energ. Fuel 37 (2023) 477–491.
[15] D. Wei, S. Han, X. Ji, T. Wang, B. Sun, J. Energy Inst. 113 (2024) 101558.
[16] L.M. Remeo, B. Pena, M. Bailera, P. Lisbona, Int. J. Hydrogen Energ. 45 (2020) 25838–25850.
[17] O. Arslan, E. Acikkalp, G. Genc, Fuel 315 (2022) 123201.
[18] X. Fu, J. Wu, Z. Sun, Y. Duan, Z. Gao, L. Duan, J. Therm. Sci. 32 (2023) 1722–1736.
[19] T. Wang, T. Zhou, Y. Feng, M. Zhang, S. Zhu, H. Yang, Appl. Therm. Eng. 242 (2024) 122513.
[20] S. Zhu, M. Zhang, B. Deng, Z. Huang, Y. Ding, G. Wang, et al., Appl. Therm. Eng. 209 (2022) 118265.
[21] A. Mehrpanahi, S.N. Naserabad, G. Ahmadi, Energy 179 (2019) 1017–1035.
[22] M. Sánchez, E. Amores, D. Abad, L. Rodríguez, C. Clemente-Jul, Int. J. Hydrogen Energ. 45 (2020) 3916–3929.
[23] Y. Wang, S. Ren, X. Che, S. Yu, J. Chen, Q. Li, W. Cai, Int. J. Hydrogen Energ. 97 (2025) 391–405.
[24] G. Sakas, A. Ibáñez-Rioja, S. Pöyhönen, A. Kosonen, V. Ruuskanen, P. Kauranen, et al., Renew. Energ. 225 (2024) 120266.
[25] C. Ge, S. Li, L. Wang, Fuel 342 (2023) 127699.
[26] M.B. Toftegaard, J. Brix, P.A. Jensen, P. Glarborg, A.D. Jensen, Prog. Energ. Combust. 36 (2010) 581–625.
[27] U. Asghar, S. Rafiq, A. Anwar, T. Iqbal, A. Ahmed, F. Jamil, J. Environ. Chem. Eng. 9 (2021) 106064.
[28] J. Yin, M. Liu, Q. Wu, J. Yan, Fuel 344 (2023) 127837.
[29] T. Liu, Y. Wang, L. Zou, Y. Bai, T. Shen, Y. Wei, Appl. Therm. Eng. 246 (2024) 122980.
[30] M. Omar, F. Yakub, R. Tasnim, F. Zhafran, A.A. Azmi, T. Morisaki, Int. J. Hydrogen Energ. 136 (2025) 339–357.
[31] B. Yang, R. Zhang, Z. Shao, C. Zhang, Int. J. Hydrogen Energ. 48 (2023) 13767–13779.
[32] H. Tebibel, in: 2018 International Conference on Wind Energy and Application in Algeria, 2018.
[33] D. Parra, M.K. Patel, Int. J. Hydrogen Energ. 41 (2016) 3748–3761.